Vacuum 167 (2019) 428–437

Contents lists available at ScienceDirect

Vacuum

journal homepage: www.elsevier.com/locate/vacuum

Shear strength and fracture behavior of solder/Kovar joints with electroplated Cu film

Xiaowu Hu[a,*], Nifa Bao[a], Qinglin Li[b]

[a] Key Lab for Robot & Welding Automation of Jiangxi Province, School of Mechanical & Electrical Engineering, Nanchang University, Nanchang, 330031, China
[b] State Key Laboratory of Advanced Processing and Recycling of Nonferrous Metals, Lanzhou University of Technology, Lanzhou, 730050, China

ARTICLE INFO

Keywords:
Shear strength
Electroplated Cu
Aging
Kovar alloy
Microstructure

ABSTRACT

In this study, the effects of isothermal aging on the interfacial reactions, shear strength and failure mode of Sn37Pb/electroplated Cu (EPC)/Kovar solder joints were investigated in detail. Various interfacial intermetallic compound (IMC) layers were formed in all as-reflowed solder joints. The as-reflowed solder joints were aged up to 360 h at 150 °C before single-lap shear tests. The microstructure of interfacial IMCs layers was affected by the isothermal aging, as well as deposited thickness of Cu film on Kovar substrate. Single-lap shear tests results revealed that the introduction of Cu film on Kovar significantly improved the shear strength of Sn37Pb/EPC/Kovar solder joints. This is because the Cu film could act as a sacrificial layer and react with molten solder to form a thin Cu-Sn IMCs layer, which was expected to protect Au/Ni films from further reaction with solder, rendering a enhanced bonding strength of joints. The shear strength of Sn37Pb/EPC/Kovar solder joints with same aging time increased first and then decreased with the increase of deposited Cu film thickness. The shear strength of aged solder joints decreased with increasing aging time, which could be ascribed to the thicker IMC layer generated at the joint interface.

1. Introduction

Kovar alloy has been widely used in electronic vacuum field for sealing-joining metals to glass because its thermal expansion coefficient is similar to that of borosilicate glass [1–3]. Wang et al. [4] bonded Kovar and SiCp/Al with Ni-P coating by using vacuum brazing. The microstructures and properties of joints were studied in detail. Song et al. [5] investigated the diffusion-bonded joints of titanium and Kovar alloy bonded by vacuum hot-press sinter and the interfacial microstructure and mechanical properties of joins were systematically studied. Lu et al. [6] had reported that the vacuum-brazed joints of SiCp/A356 MMCs and Kovar connected by using Zn-58Cd-2Ag-2Cu solder had displayed a good reliability. However, they found these joints were easily corroded. It is well known that the corrosion resistance and solderability of Kovar alloy were so poor. Thus, the Kovar alloy is plated with thin Ni layer to enhance its corrosion resistance and then gold to improve its solderability [7–10]. A series of works had been detailly studied on the Kovar alloy with Ni/Au plating in soldering [11–14]. Lopez et al. [11] studied the solderability of SnAgCu/Au-Ni-plated Kovar solder joints, the result showed that the Au-Ni surface could effectively improve the solderability of Kovar alloy. Yoon et al. [12] had investigated the interfacial reaction at the interface between Au-Sn solder and Kovar alloy. However, a limited number of works have been investigated on the interface reaction and microstructure evolution of interface between Sn-based solder and Kovar substrate.

The mechanical properties are the crucial parameters to reflect the reliability of solder joints for electronic packaging industry [15–17]. In order to evaluate the mechanical properties of solder joints, it is most common to perform bond strength test. Thus, the bond strength of solder joints was one of major research area in electronic packaging field [18]. As well known, the intermetallic compound (IMC) appears at the interface between solder alloy and substrate during soldering, which is an important sign of good interconnection [19]. Furthermore, the interfacial IMC layer of solder joint is also closely related to its bond strength [20]. Hu et al. [21] had performed the single-lap shear test, the results revealed that the interfacial IMC layer thickness of solder joints increased obviously with increasing aging time, while the shear strength decreased. In the work of Ahat et al. [22], the effects of aging on the microstructure and shear strength of SnAg/Cu solder joints were studied. It was found that the shear strength also decreased as the aging time increased. Based on previous researches, it is obvious that the interfacial IMC layer thickness and microstructure of solder joint could be significantly controlled by aging during service. A large number of existing researches on the mechanical properties of solder joints are

* Corresponding author.
E-mail address: huxiaowu@ncu.edu.cn (X. Hu).

https://doi.org/10.1016/j.vacuum.2019.07.002
Received 23 April 2019; Received in revised form 19 May 2019; Accepted 1 July 2019
Available online 02 July 2019
0042-207X/

focused on Sn-based solder/Cu joints, Sn-based solder/Ni joints and so on. As for soldered Sn-based/Kovar joints, the researches on the effect of thermal aging on microstructure and mechanical properties of this joints had rarely been found in the past. Hence, it is essential to investigate the effect of isothermal aging on interfacial IMC layer formed at the interface of Sn-based solder and Kovar substrate.

According to our previous study [23], it can be found that the introduction of a electroplating Cu (EPC) layer as a sacrificial layer on the surface of Kovar alloy could significantly improve the reliability of Sn-based/EPC/Kovar solder joints, but the effect of thermal aging and deposit thickness on the shear strength of Sn-based/Kovar joint had not investigated in detail. The effects of deposit thickness on the interfacial reaction and microstructure of solder joint were reported in some previous studies, it should be noted that the different deposit thickness on the surface of substrate also has a great influence on the microstructure and reliability of solder joints. Yu et al. [24] had found that the thicker deposit Cu film, the more impurities and vacancies during aging. Ho et al. [25] reported that the Pd(P) thickness had strong effect on the interfacial reaction of SnAgCu/Au/Pb(P)/Ni(P)/Cu solder joints. Hence, this paper had systematically investigated the microstructure and mechanical properties of soldered Sn-based/EPC/Kovar joints with different deposit thickness during isothermal aging.

Although Sn37Pb solder has been almost replaced by lead-free solder out of environmental concerns, it is still used in some areas, such as military and aerospace industries, due to its excellent soldering and mechanical properties. Chaffarian et al. [26] showed that the solder joint with Sn37Pb solder could be good serviced after 200 thermal cycles compared to other lead-free solders. The European Commission (EC) has also exempted solder joints requiring high performance support from the use of Tin-lead solders, which is ascribed to the need to maintain the solder joints reliability and operational integrity in certain electronic products [27]. In this work, in order to obtain the solder/Kovar joints with good comprehensive performance, the Sn37Pb/EPC/Kovar solder joints are employed to reveal the effects of aging on microstructure and reliability of solder joint.

2. Experimental procedures

In this paper, the commercial Sn37Pb (wt. %) solder paste (KOKL, Korea) was used as solder. The Kovar plate (Zhaozhan Metal Materials Co. Ltd, China) was prepared by means of injection molding, in which the raw alloy was first hot defatted in a vacuum defatting furnace and then sintered in a vacuum sintering furnace (a favorable vacuum atmosphere is necessary at injection molding processing [28]). Besides, the Kovar substrare was plated with 4.1 μm thick Ni and 1.9 μm thick Au films, which used as the substrate. The Kovar substrate was carefully cleaned with acetone solution in ultrasonic oscillator after being processed to the dimensions of 8 mm × 20 mm × 0.3 mm. Then the cleaned Kovar plates were electroplated with a thin Cu layer. The electroplating solution was a traditional copper sulfate electroplating solution. The current density was 2 A/dm^2 and the temperature of Cu plating bath was about 40 °C. It could be found from the prepared Kovar plates that the average thickness of electroplated Cu layers were about 1.0, 2.9, 4.0 and 6.5 μm after electroplating for 2, 5, 10 and 20 min, respectively. The most common test method for mechanical properties of solder joint is the single-lap shear test [21]. Thus, the single-lap shear specimen was used to simulate the actual solder joint in this study, as shown in Fig. 1. The printing machine was used to coat the prepared substrate with Sn37Pb solder paste to ensure the dimension uniformity of the solder joints. Besides, two same aluminum spacers were also placed on both sides of the Sn37Pb solder paste to ensure a uniform joint thickness. The thickness of aluminum spacer was about 150 μm, which was same to that of the printed stencil. Subsequently, the single-lap samples made according to the model shown in Fig. 1, were placed into an reflow furnace. The reflow temperature was 250 °C and the reflow time was 300 s. The single-lap shear samples were subjected to isothermally aged at 150 °C up to 360 h.

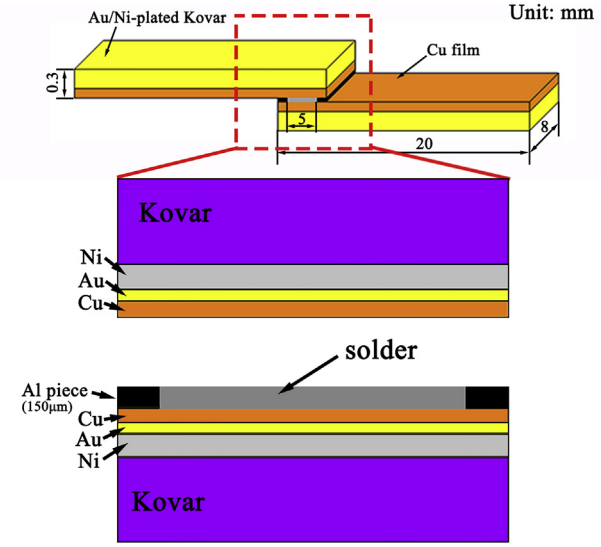

Fig. 1. Schematic illustration of Sn37Pb/EPC/Kovar joint shear sample, (unit: mm).

In order to examine the shear strength of the solder joints, the shear tests were performed by using a uniaxial micro-force test system. The tests were carried out at room temperature and with a constant strain rate of 2.5 × 10^{-2} s^{-1}. An average value in shear force was taken from at least five samples under each experimental condition.

To examine the microstructure and fracture behavior of solder joint, the metallography and corresponding fracture surfaces of samples were observed by using a Scanning Electron Microscope (SEM, FEI Quanta200F). An Energy Dispersive Spectrometer (EDS) analysis was conducted to qualitatively determine the compositions of the IMCs of solder joints. Furthermore, the surface morphology of deposited Cu film was obtained by the atomic force microscope (AFM, XE-100, Park System) analysis.

3. Results and discussion

In order to investigate the surface morphologies of deposited Cu film, the AFM tests were performed on the electroplated Cu film with an area of 100 × 100 μm^2. Fig. 2 shows the AFM micrographs of Cu film. The deposited thicknesses of Cu films were 1.0, 2.9, 4.0 and 6.5 μm, respectively. The surface roughness values (R_a) and maximum height difference (p-v) of deposited Cu film were also listed in Table 1. When the deposited Cu film thickness was 1.0 μm, as shown in Fig. 2a, the Ra and p-v were about 200.5 and 1.96 × 10^3 nm, respectively. They increased to 254.6 and 3.92 × 10^3 nm with the deposited Cu film thickness of 6.5 μm. It could be suggested that the Ra of Cu film tends to increase with increasing thickness of Cu film. The higher surface roughness with the thicker Cu film might be attributed to the formation of irregular and larger Cu particles on the plating surface during the continuous electro-deposition.

Fig. 3 shows the cross-sectional SEM images of Sn37Pb/EPC/Kovar solder joints reflowed at 250 °C for 300 s. The deposited thicknesses of Cu films were 0, 1.0, 2.9, 4.0 and 6.5 μm, respectively. Various interfacial IMC layers were formed in all as-reflowed solder joints. When the Kovar substrate was without copper plating, it can be seen from Fig. 3a that the Au layer on Kovar disappeared in the as-reflowed joint [29], indicating that the Au atoms dissolved rapidly into molten solder matrix during soldering. As a result, a number of Au-Sn binary IMCs and Au-Sn-Ni ternary IMCs were formed within the solder matrix and at the joint interface. For instance, a single (Ni, Au)$_3$Sn$_4$ IMC layer covered with a intermittent (Au, Ni)Sn$_4$ IMC layer, was formed on Ni layer, as

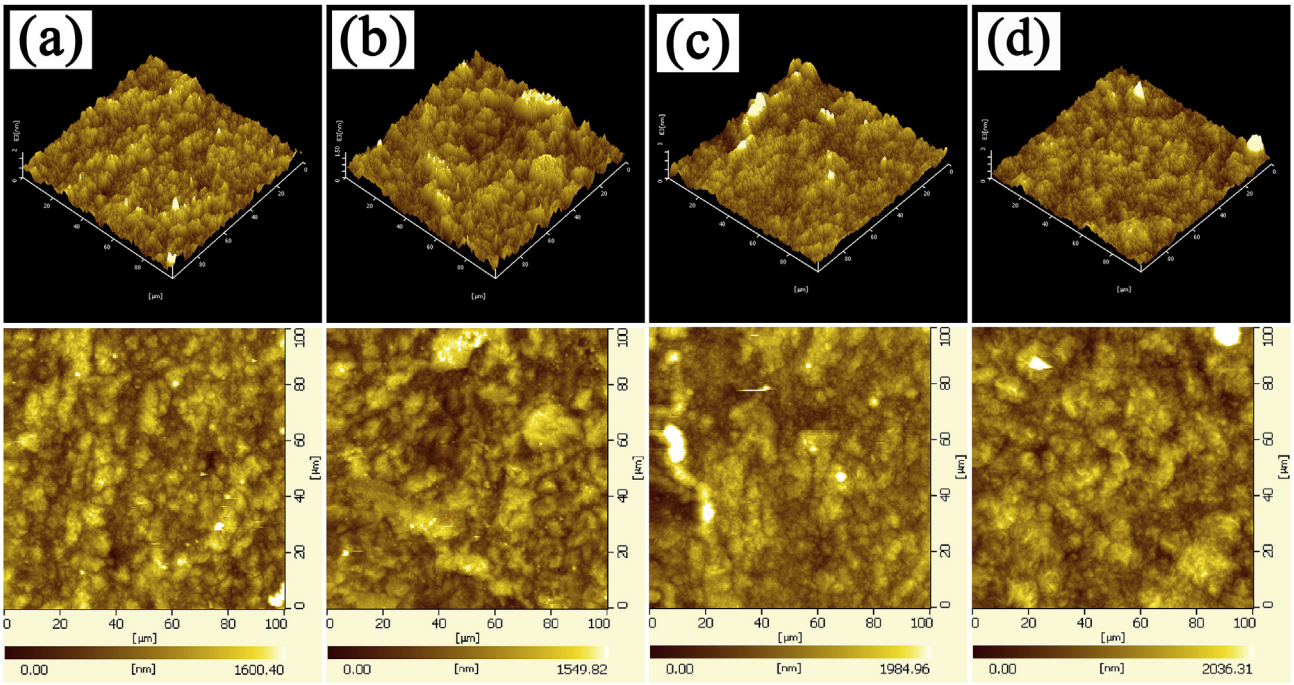

Fig. 2. AFM micrographs of Cu film surface prepared by different deposit thicknesses during electroplating, (a) 1.0 μm, (b) 2.9 μm, (c) 4.0 μm, (d) 6.5 μm.

Table 1
The surface roughness (R_a) and maximum height difference (p-v) of Cu films with different deposited thicknesses..

The thickness of Cu film (μm)	1.0	2.9	4.0	6.5
R_a (nm)	200.5	210.6	244.4	254.6
p-v (nm)	1.96×10^3	2.62×10^3	3.18×10^3	3.92×10^3

Table 2
EDS analysis results of phases formed at Sn37Pb/Kovar solder joint, shown in Fig. 3a.

	Ni (at. %)	Au	Sn	Intermetallic
Spectrum 1	28.23	13.53	58.25	$(Ni, Au)_3Sn_4$
Spectrum 2	7.05	16.28	76.67	$(Au, Ni)Sn_4$
Spectrum 3	–	32.84	67.16	$AuSn_2$
Spectrum 4	–	20.29	79.71	$AuSn_4$

shown in Fig. 3a. Besides, numerous Au-Sn ($AuSn_2$ and $AuSn_4$) binary IMCs were also observed in the solder matrix. The EDS analysis was performed in the selected areas of Fig. 3a and the results were listed in Table 2. According to the EDS analysis results, the spectrum 1 indicated that the interfacial IMC layer near to Kovar consisted of 28.23% Ni, 13.53% Au and 58.25% Sn, which was identified to be $(Ni, Au)_3Sn_4$ phase. The spectrum 2 represented that the intermittent IMC layer was $(Au, Ni)Sn_4$ phase, consisting of 7.05% Ni, 16.28% Au and 76.67% Sn. Furthermore, it was clear that the Sn37Pb solder was composed of Sn-rich phase and Pb-rich phase, as shown in Fig. 3a. As the deposited Cu film thickness was 1.0 μm, as shown in Fig. 3b, similar to the solder joints without electroplating Cu, the Au layer disappeared completely

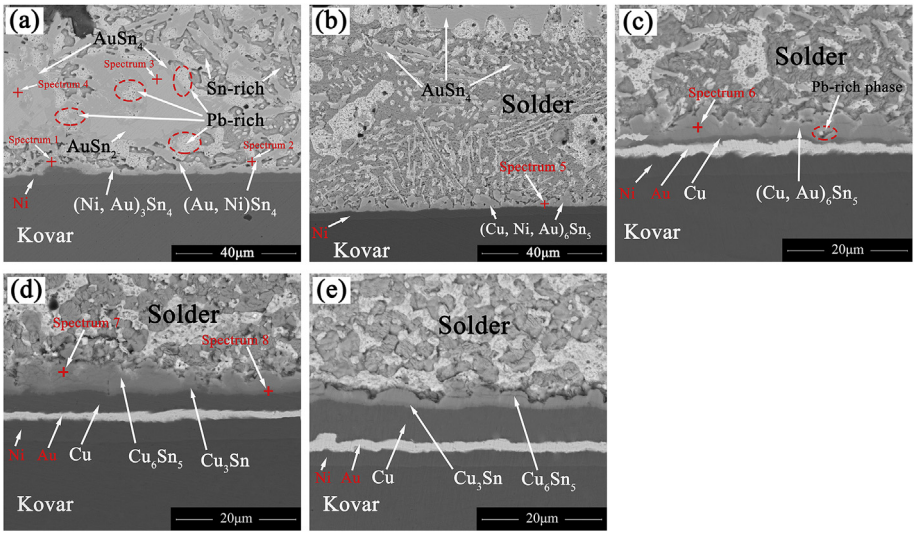

Fig. 3. Cross-sectional SEM images of as-reflowed solder joints with various deposited thicknesses of Cu film, (0) 0 μm, (b) 1.0 μm, (c) 2.9 μm, (d) 4.0 μm and (e) 6.5 μm.

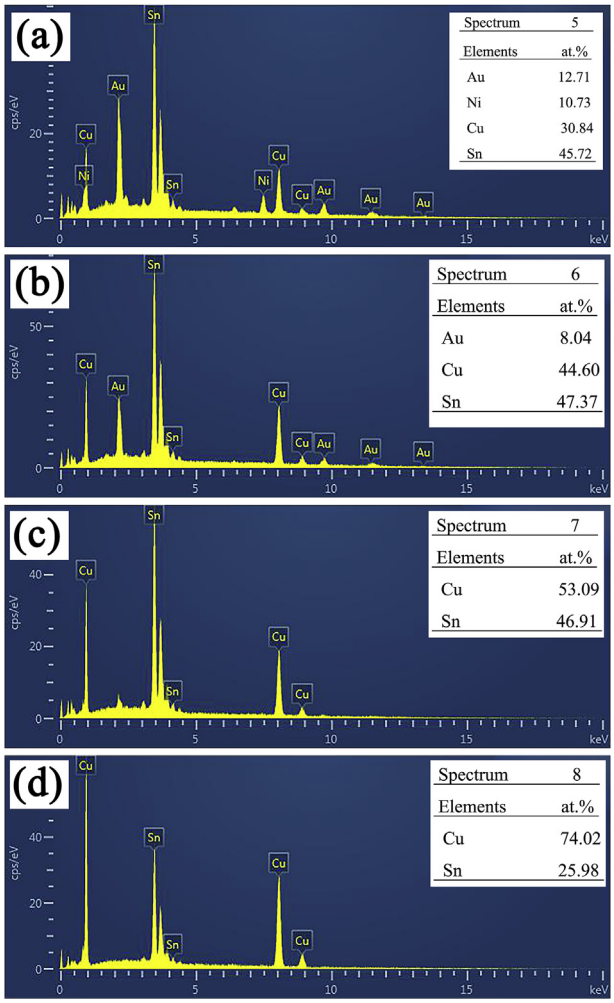

Fig. 4. EDS results of IMCs in Fig. 3b–d, (a) Spectrum 5, (b) Spectrum 6, (c) Spectrum 7 and (d) Spectrum 8.

from joint interface. In addition, the deposited Cu film was consumed totally. Due to the introduction of electroplated Cu film, the interfacial reaction products of solder joints were transformed from (Ni, Au)$_3$Sn$_4$ phase to (Cu, Ni, Au)$_6$Sn$_5$ phase. The EDS analysis results indicated that the interfacial IMC layer was indeed (Cu, Ni, Au)$_6$Sn$_5$ IMC layer, as shown in Fig. 4a. According to previous studies [30,31], the Au and Ni atoms were able to dissolve in Cu$_6$Sn$_5$ by replacing Cu atoms during soldering, lead to the formation of (Cu, Ni, Au)$_6$Sn$_5$ phase at the joint interface.

As the deposited thickness of Cu film was 2.9 μm, an obvious change was observed at the joint interface. The entire Au layer and unreacted Cu film were retained at the interface of solder joint. The original product was (Cu, Au)$_6$Sn$_5$ IMC, consisting of 44.60% Cu, 8.04% Au and 47.37% Sn, as show in Fig. 3c. It was indicated that only a small number of Au atoms passed through the Cu layer and reacted with Sn atoms and Cu atoms at the interface during the soldering process. Interestingly, some Pb-rich phases were found inside IMC and most of IMCs were surrounded by Pb-rich phase, as marked by red circle in Fig. 3a and c. This phenomenon could be explained by the fact that a large number of Sn-rich phases in Sn37Pb solder reacted with Au, Cu and Ni atoms, resulting in that the Pb-rich phases clustered around IMCs. Further increasing the deposited thicknesses of Cu film to 4.0 μm and 6.5 μm, due to sufficient thickness of Cu film, a certain thickness of Cu film remained at the interface of as-reflowed solder joint. Hence, a typical bi-layer IMC consisting of the scallop-shaped Cu$_6$Sn$_5$ IMC (solder side) and the planar Cu$_3$Sn IMC (Kovar side) was found at the interface, as shown in Fig. 3d and e. It was well known that there are three interfacial reactions between the solder and Cu substrate, described by the following equations [18,32]:

$$6Cu + 5Sn = Cu_6Sn_5 \quad (1)$$

$$3Cu + Sn = Cu_3Sn \quad (2)$$

$$9Cu + Cu_6Sn_5 = 5Cu_3Sn \quad (3)$$

Meanwhile, the Au film and Ni layer could be also observed. The EDS analysis was conducted for selected spectrums 6–8 in Fig. 3c and d. The results were shown in Fig. 4b–d, respectively. In a word, it was clearly indicated that the introduction of Cu layer with different thicknesses on Kovar substrate has a significant impact on the composition and microstructure of interfacial IMC layers of solder joints.

Fig. 5 shows the SEM images of Sn37Pb/Kovar solder joints aged at 150 °C for various aging duration. Compared to the interfacial IMC layer of as-reflowed solder joint, a similar IMC layer microstructure composed of (Au, Ni)Sn$_4$ and (Ni, Au)$_3$Sn$_4$ IMC was found at the interface of solder joint aged for 24 h, but the total IMC thickness increased from 2.11 μm to 4.25 μm, as shown in Fig. 5a. With the further extension of isothermal aging time, the thickness of interfacial IMC layer increased continuously. Besides, the types of interfacial IMCs did not change but the thickness of (Ni, Au)$_3$Sn$_4$ IMC layer grew rapidly, as illustrated in Fig. 5b–d. Furthermore, a large number of Au-Sn IMCs were detected in the solder matrix in Fig. 5c and d. The Ni layers still remained at the interfaces of all aged joints.

Fig. 6 shows the SEM images of aged Sn37Pb/EPC/Kovar solder joints with 2.9 μm thickness of Cu deposited film. Fig. 6a shows the interfacial microstructure of solder joint aged for 24 h. It can be seen that a very thin Cu layer still remained on the Au layer. Moreover, only a single (Cu, Au)$_6$Sn$_5$ IMC layer was clearly observed at the aged joint interface. There was a difference, no significant compound formation was observed in the solder matrix, from the solder joint without electroplating Cu treatment. This indicated that the existence of Cu film greatly reduced the diffusion of atoms in the interface reaction, resulting in that the Au atoms slowly dissolved into the solder matrix to form Au-Sn IMCs. Further increase the aging time to 120 h, the deposited Cu film gradually completely consumed during following aging process. Then a tri-layer consisting of (Cu, Au)$_6$Sn$_5$ phase near to solder, (Cu, Au)$_3$Sn phase near to Kovar and Cu$_3$Sn phase between them was seen in Fig. 6b. The IMCs were identified by EDS analysis and the results were listed in Table 3. In addition, it was clear that the thickness of interfacial IMCs layers increased with the increase of isothermal aging time.

Fig. 7 shows the SEM images of Sn37Pb/EPC/Kovar solder joints with 6.5 μm deposited Cu film aged at 150 °C for various aging duration. The thickness of Cu film became gradually thinner during aging process, as a result, a double-layer, which was composed of Cu$_6$Sn$_5$ phase and Cu$_3$Sn phase, was observed at the aged joint interface, as shown in Fig. 7a–d. The EDS analysis results were shown in Fig. 8a and b. It is suggested that a sufficient thickness of Cu layer existed between the solder and substrate effectively prevented the diffusion of Au atoms toward Sn-based solder during soldering, leading to the formations of the Cu$_6$Sn$_5$ phase and Cu$_3$Sn phase at the interfaces of aged solder joints. It was noticed that some voids were found near the Cu$_3$Sn/Cu interface in all aged joints, as marked by red circles in Fig. 7a–d. These voids were identified to be Kirkendall voids, which were formed due to the unbalanced diffusion between atoms in reflow process [33]. Thus, the longer aging time would result in more voids. Moreover, a large number of Kirkendall voids were observed in the Cu$_3$Sn IMC layer and then accumulated together to form cracks, which seriously deteriorated the reliability of the solder joints. It is worthy noticed that some cracks through the whole IMC layer were appeared, was indicated in Fig. 7a–d. This phenomenon could be explained by the inherent brittleness of IMC [34]. Additionally, similar cracks were also observed in Fig. 6d.

As is well known that the solder joints in electronic packaging field

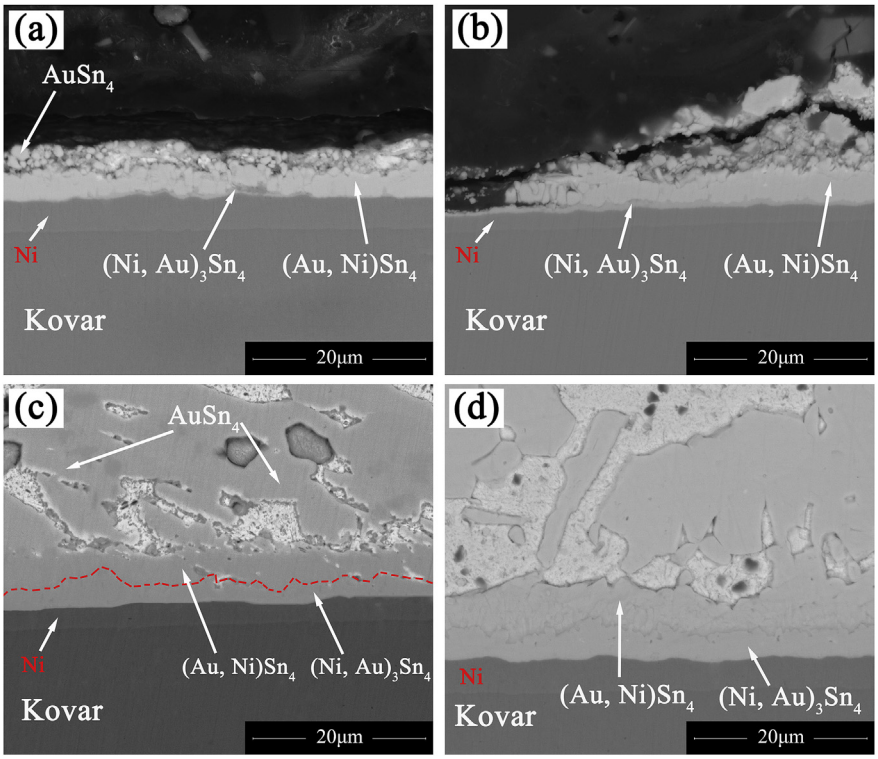

Fig. 5. Cross-sectional SEM images of Sn37Pb/Kovar system after aging at 150 °C for various time, (a) 24 h; (b) 120 h; (c) 240 h and (d) 360 h.

are always confronted with high temperature condition in service. To evaluate the thermal stability of solder joints with different deposited thickness of Cu film, the samples were subjected to shear tests after thermal aging. The results were displayed in Fig. 9, which showed the shear strength of all single-lap Sn37Pb/EPC/Kovar solder joints aged for various time. It was clearly indicated that the shear strength of aged solder joints decreased with increasing aging time. As above mentioned, the interfacial IMC layer grew in thickness during the solid-state isothermal aging process. A relatively thick IMC layer formed at the joint interface could greatly reduce the solder joint reliability, which was

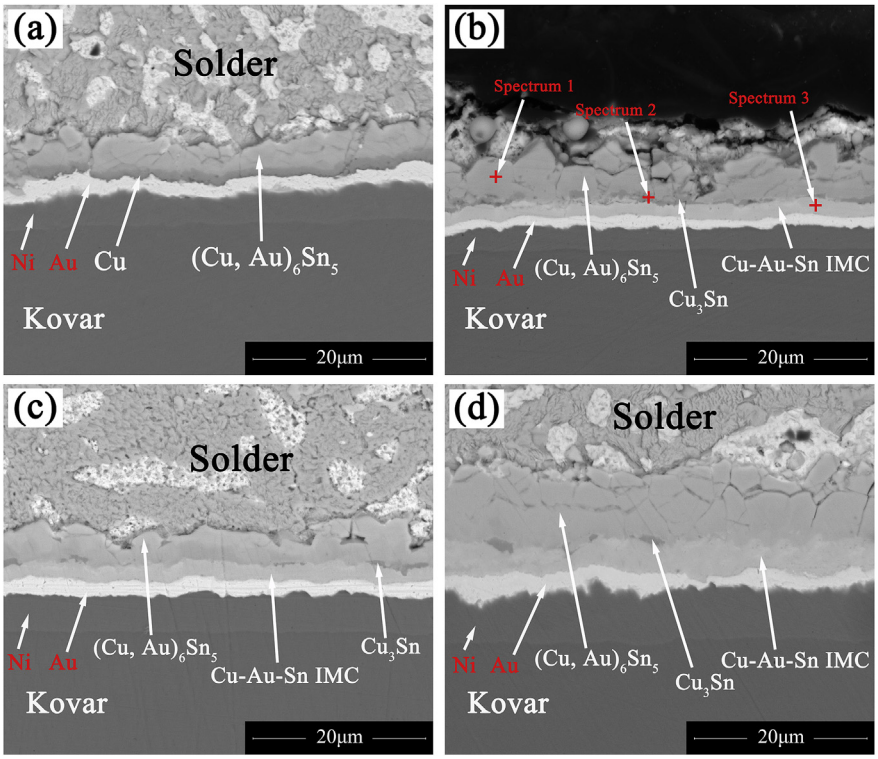

Fig. 6. Cross-sectional SEM images of Sn37Pb/EPC/Kovar system after aging at 150 °C for various time, (a) 24 h; (b) 120 h; (c) 240 h and (d) 360 h; the deposited thickness of Cu film was 2.9 μm.

Table 3
EDS analysis results of phases formed at Sn37Pb/EPC/Kovar solder joint, shown in Fig. 6b.

	Cu (at. %)	Au	Sn	Intermetallic
Spectrum 1	47.59	4.09	48.32	$(Cu, Au)_6Sn_5$
Spectrum 2	75.58	–	24.42	Cu_3Sn
Spectrum 3	54.46	23.66	21.88	$(Cu, Au)_3Sn$

attributed to the inherent brittleness and the tendency to generate structural defects of interfacial IMC layer. Numerous previous investigations reported that the excessive IMCs growth could deteriorate solder joint microstructure and weaken its strength, and thus affect the reliability of solder joint in long-term service [35,36]. Hence, it can be concluded that the reduction in shear strength of Sn37Pb/EPC/Kovar solder joints could be ascribed to the thick IMC layer generated at the joint interface. This conclusion was consistent with the previous study proposed by Hu et al. [34], who found the shear strength of SAC305/Cu joint decreased as the increase of interfacial IMC layer thickness and aging time.

Besides, it could be seen from Fig. 9 that the shear strengths of all samples with electroplated Cu film were higher than that of samples without electroplating Cu film. Thus, it was suggested that the introduction of Cu film on Kovar substrate for solder joints reliability was positive and effective. The plausible reason why the introduction of Cu film on Kovar could significantly improve the shear strength of Sn37Pb/EPC/Kovar joints was stated as follows: The Cu film was electroplated on Kovar substrate as a diffusion barrier to suppress the interfacial reaction and the formation of IMCs. This is because the Cu film can react with molten solder to form Cu-Sn IMCs layer between the solder and substrate, thereby reducing the interfacial reaction rate and enhancing the solder joint reliability. This phenomenon has also been proposed in previous work [37]. Lee et al. [37] enhanced the solder joint strength by employing an Cu film deposited on Ni layer to prevent a full-scale materials interaction. In addition, the shear strength increased first and

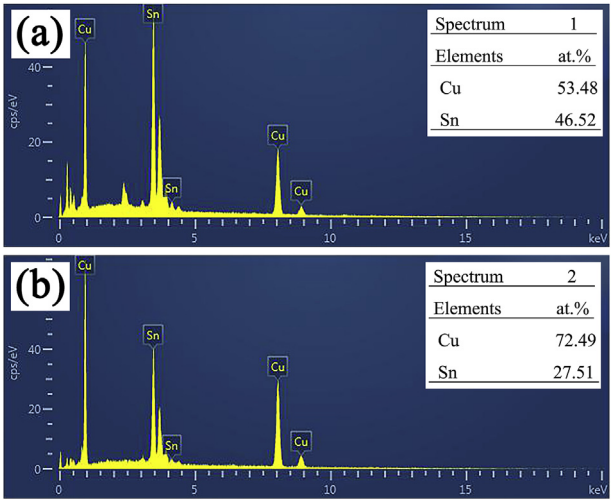

Fig. 8. EDS results of IMCs in Fig. 7a, (a) Spectrum 1 and (b) Spectrum 2.

then decreased with the increase of deposited Cu film thickness of solder joints under the same experiment condition. This phenomenon has been explained in our previous work [23]. The thickness of interfacial IMCs layers in the solder joint had a significant effect on its shear strength [38]. It was suggested that the thicknesses of interfacial IMCs layers in Sn37Pb/EPC/Kovar solder joints were affected by the deposited Cu film thickness on the Kovar substrate. The thicknesses of interfacial IMCs layers of all as-reflowed solder joints were measured and at least five samples values were average. The results were listed in Table 4. It can be clearly found from Table 4 that the thickness of interfacial IMC layer of as-reflowed solder joint increased first and then decreased with the increase of deposited Cu film thickness, which was in accordance with the changing trend of solder joint strength. Hence, the changes of solder joint strength could be explained by the various

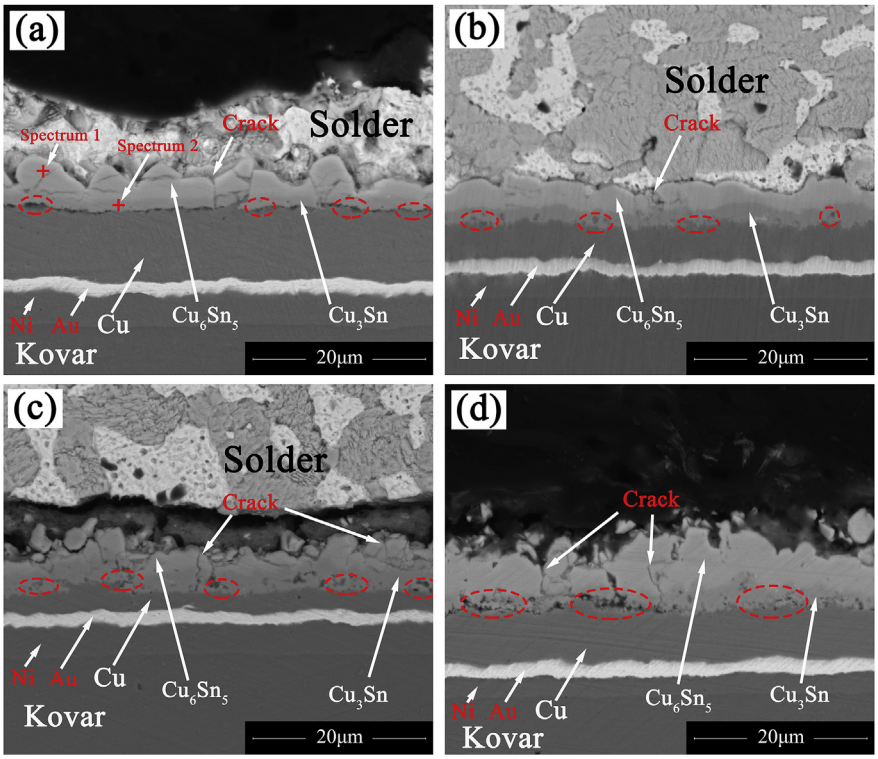

Fig. 7. Cross-sectional SEM images of Sn37Pb/EPC/Kovar system after aging at 150 °C for various time, (a) 24 h; (b) 120 h; (c) 240 h and (d) 360 h; the deposited thickness of Cu film was 6.5 μm.

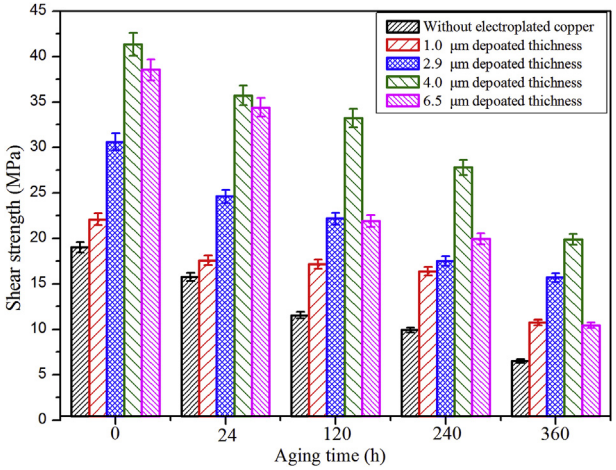

Fig. 9. Shear strength of solder joints aged at 150 °C for various time.

Table 4
The interfacial IMC thicknesses of as-reflowed solder joints with different deposited thicknesses of Cu films.

Deposited thickness of Cu film (μm)	1.0	2.9	4.0	6.5
The thickness of IMC layer (μm)	2.57	3.31	3.76	2.78

thickness of the interfacial IMC layer.

As is well known that the failure modes of solder joints under shear loading conditions could be divided into three types according to the different fracture locations, including solder mode, mixed solder/IMC mode and IMC mode [3]. Fig. 10a schematically illustrates the fracture positions of solder joints under three different fracture modes. For "solder" fracture mode, both the formation and propagation of crack occurred within the solder matrix. It was seen that the shear fracture surface was full of residual solder, as shown in Fig. 10b1 and b2. For the "mixed solder/IMC" fracture mode, the fracture crack propagated across the solder matrix and partly inside the IMC layer. Both the solder and IMC were observed on the fracture surface, as shown in Fig. 10c. For the "IMC" fracture mode, the fracture crack mainly yielded in the IMC layer, but it also could pass through the solder/IMC or IMC/substrate interface, as shown in Fig. 10d.

In order to investigate the fracture behavior of Sn37Pb/EPC/Kovar solder joints after isothermal aging process, the cross-sectional fracture morphologies and shear fracture surfaces of solder joints were examined by using SEM, as displayed in Figs. 11–13. Fig. 11 shows the cross-sectional fracture morphologies and corresponding shear fracture surfaces of Sn37Pb/Kovar solder joints. Fig. 11 a and b were the respective SEM images of solder joints aged for 0 and 240 h. It was clearly indicated that the fracture surfaces of both two joints were composed of solder and IMCs, indicating that both solder joints failed with "mixed solder/IMC" fracture mode, as shown in Fig. 11a2 and b2. However, the fracture surface was mainly covered by solder and only a small amount of IMC could be detected after soldering, as shown in Fig. 11a1 and a2. In addition, some dimples were found within the broken solder matrix, which indicated that a large amount of plastic deformation occurred in the solder matrix during the shearing process. The dimples are a typical feature of ductile fracture [39]. Hence, the failure of this joint was dominated by ductile fracture. In contrast, the fracture crack was mainly observed within the IMC layer as the solder joints was aged for 240 h, as shown in Fig. 11b1. Due to the inherent brittleness of IMC layer, it was easy to understand that the failure of aged Sn37Pb/Kovar solder joints was dominated by brittle fracture. The reason why the failure modes of Sn37Pb/Kovar solder joints changed from ductile fracture dominant to brittle fracture dominant could be attributed to the change of strength and ductility in the solder, which has been reported by Lee et al. [35].

Fig. 12 shows the cross-sectional fracture morphologies and corresponding shear fracture surfaces of Sn37Pb/EPC/Kovar solder joints with 1.0 μm thickness of deposited Cu film aged at 150 °C for 0 and 240 h, respectively. Both solder and IMC were detected on the fracture surface of as-reflowed solder joint in Figs. a1-a2, indicating that the as-reflowed solder joint failed with "mixed solder/IMC" fracture mode. In this case, due to the solder being pulled out, more IMC was exposed to the fracture surface than that of solder joint without Cu plating. Fig. 12b1-b2 show the cross-sectional fracture morphologies and corresponding fracture surfaces of aged Sn37Pb/EPC/Kovar solder joints. It can be observed that the fracture surface was completely covered by the IMC, which showed that the failure mode of the aged solder joint was "IMC" fracture mode. Additionally, there were some cracks found within the (Cu, Ni, Au)$_6$Sn$_5$ IMC layer on the fracture surface, as illustrated in Fig. 12b2. This phenomena could be explained by the natural brittleness of the IMC layer, which was consistent with the works of Hu et al. [34], who reported that the thicker IMC layer leads to a higher sensitivity of crack propagation.

Fig. 13 shows the cross-sectional fracture morphologies and corresponding shear fracture surfaces of Sn37Pb/EPC/Kovar solder joints with 4.0 μm thickness of deposit Cu film aged at 150 °C for 0 and 240 h, respectively. Fig. 13a1 shows that the typical bi-layer IMC composed of Cu_6Sn_5 and Cu_3Sn IMCs layers, which was completely covered with Sn37Pb solder, was detected at the interface of as-reflowed solder joint after shear test. Accordingly, it was seen from Fig. 13a2 that the

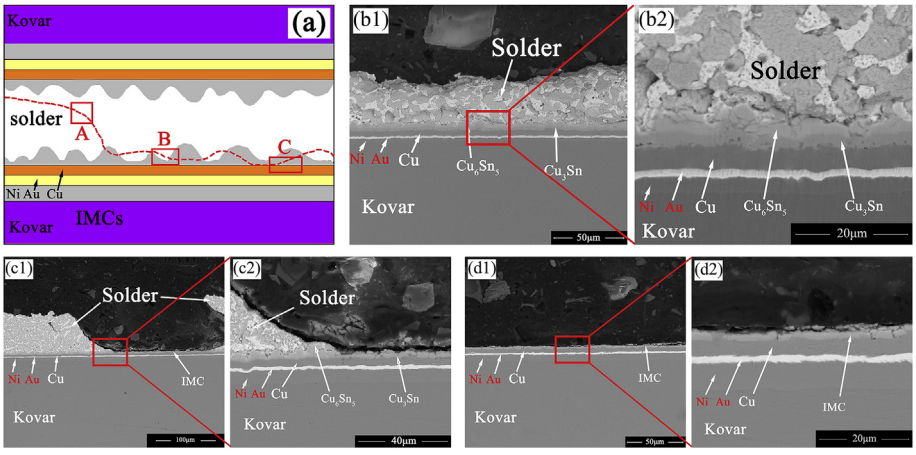

Fig. 10. The schematic illustration of three different fracture modes. (a) schematic illustration; (b1-b2) SEM images of solder mode of square A in (a); (c1-c2) SEM images of mixed solder/IMC mode of square B in (a) and (d1-d2) SEM images of IMC mode of square C in (a).

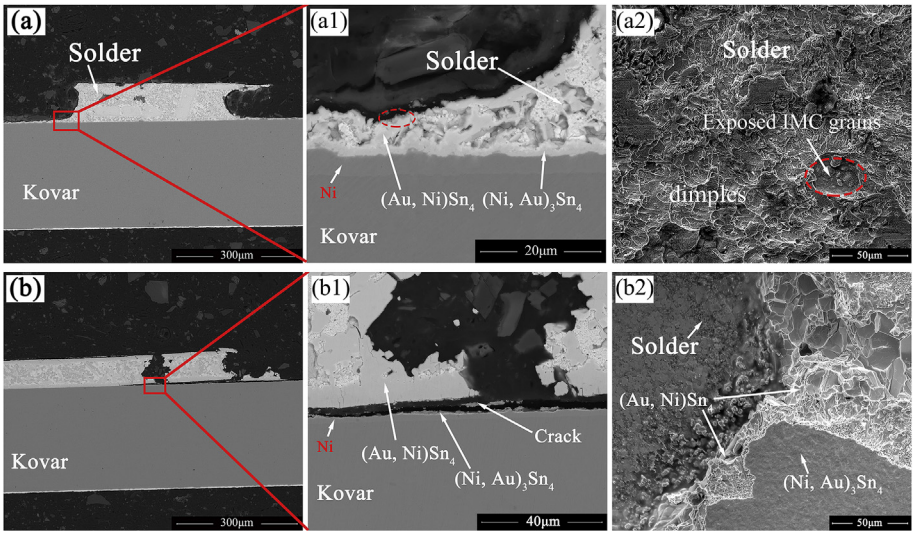

Fig. 11. Cross-sectional fracture morphologies of Sn37Pb/Kovar solder joints aged at 150 °C for (a) 0 and (b) 240 h; (a1-a2) and (b1-b2) are the enlargements SEM images of selected areas indicated by the red square in (a) and (b), correspondingly. (For interpretation of the references to colour in this figure legend, the reader is referred to the Web version of this article.)

fracture surface was entirely covered with solder and a number of ductile dimples were clearly observed, indicating that the as-reflowed solder joint in this case failed with "solder" fracture mode. After longer aging, the fracture crack occurred within IMC layer and the fracture surface was covered by Cu_3Sn IMC, as shown in Fig. 13 b1 and b2. Hence, it was confirmed that the fracture path was generated and extended within interfacial IMC layer and the aged solder joint in this case failed with "IMC" fracture mode. There are three important effects of aging on this phenomenon that the change of solder joint failed with "solder" fracture mode to "IMC" fracture mode: (a) The thicker IMC layer leads to a higher sensitivity of crack propagation due to the natural brittleness of IMC; (b) The higher percentage of Cu_3Sn in interfacial IMC layer, resulting in that the interfacial delamination played a dominant role in the fracture mode of solder joints due to the difference in fracture toughness [40]; (c) more Kirkendall voids formed at the interfaces of Cu_3Sn/Cu and Cu_6Sn_5/Cu_3Sn tended to aggregate and became cracks, which severely deteriorated the reliability of solder joints [18]. In summary, the failure mode of solder joint was directly changed by the long-term aging treatment. Moreover, the crack was appeared in the Cu_3Sn IMC layer in Fig. 13b2, which was consistent of the phenomenon observed in Fig. 7. It can be also explained by the inherent brittleness of IMC.

4. Conclusions

In summary, the interfacial reactions, shear strength and failure mode of Sn37Pb/EPC/Kovar solder joints aged at 150 °C for various time were investigated. Based on the present research, the following conclusions can be drawn:

(1) The introduction of Cu layer with different thicknesses on Kovar substrate has a significant impact on the composition and microstructure of interfacial IMC layers of solder joints. Comparing with solder joint without electroplated Cu, a typical bi-layer IMC consisting of the scallop-shaped Cu_6Sn_5 IMC (solder side) and the planar Cu_3Sn IMC (Kovar side) was found at the joint interface as the deposited thicknesses of Cu film increase to 4.0 μm,.
(2) The introduction of Cu film on Kovar obviously improved the shear strength of Sn37Pb/EPC/Kovar solder joints. This was because the Cu film could act as a sacrificial layer and react with molten solder to form Cu-Sn IMCs layer between the solder and substrate, which was expected to protect Au/Ni films from further reaction with solder, rendering a enhanced bonding strength of joints.
(3) The shear strength of Sn37Pb/EPC/Kovar solder joints with same aging time increased first and then decreased with the increase of deposited Cu film thickness. This phenomenon can be explained by the thickness of interfacial IMCs layer in the solder joint had a

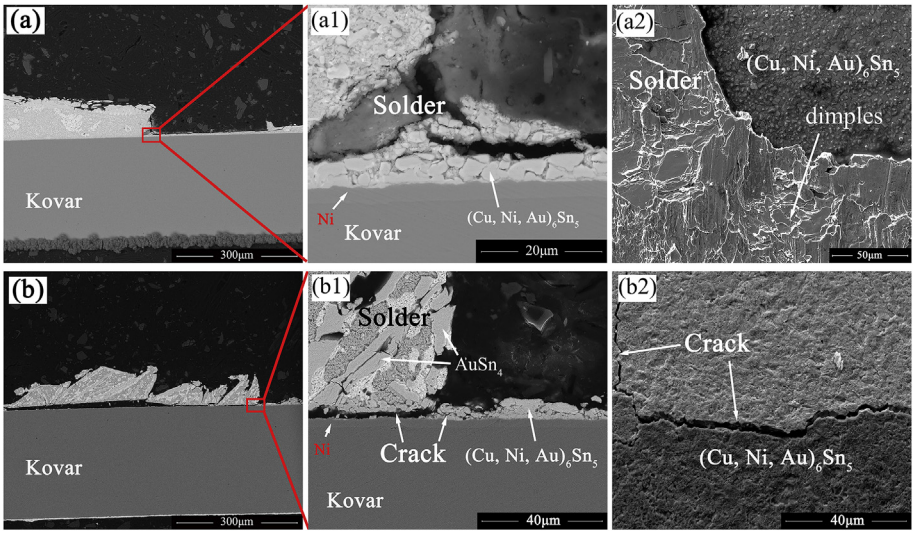

Fig. 12. Cross-sectional fracture morphologies of Sn37Pb/EPC/Kovar solder joints aged at 150 °C for (a) 0 and (b) 240 h; The deposited Cu film thickness was 1.0 μm; (a1-a2) and (b1-b2) are the enlargements SEM images of selected areas indicated by the red square in (a) and (b), correspondingly. (For interpretation of the references to colour in this figure legend, the reader is referred to the Web version of this article.)

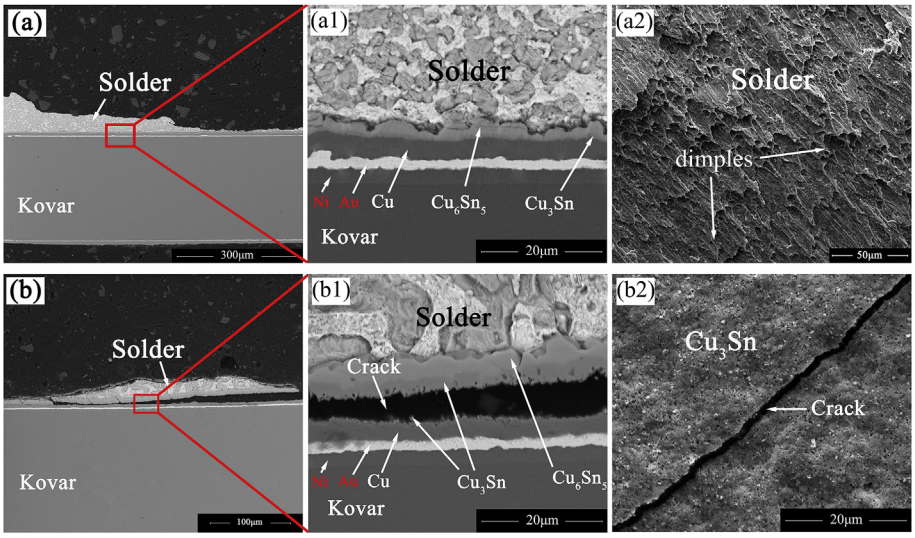

Fig. 13. Cross-sectional fracture morphologies of Sn37Pb/EPC/Kovar solder joints aged at 150 °C for (a) 0 and (b) 240h; The deposited Cu film thickness was 4.0 μm; (a1-a2)and (b1-b2) are the enlargements SEM images of selected areas indicated by the red square in (a) and (b), correspondingly. (For interpretation of the references to colour in this figure legend, the reader is referred to the Web version of this article.)

significant effect on its shear strength. The shear strength of aged solder joints decreased obviously with increasing aging time, which could be ascribed to thicker interfacial IMC layer leads to a higher sensitivity of crack propagation.

(4) After long-term aging treatment, the failure modes of Sn37Pb/Kovar solder joints changed from ductile fracture dominant to brittle fracture dominant, which was attributed to the change of strength and ductility in the solder. Furthermore, three important factors that lead to the change of Sn37Pb/EPC/Kovar solder joints with 4.0 μm thickness of deposited Cu film in fracture mode from "solder" fracture mode to "IMC" fracture mode: the thicker IMC layer, the higher percentage of Cu_3Sn in interfacial IMC layer and more Kirkendall voids formed at the interfaces of Cu_3Sn/Cu and Cu_6Sn_5/Cu_3Sn.

Acknowledgement

This work was supported by the National Natural Science Foundation of China (No. 51765040), Natural Science Foundation of Jiangxi Province (20161BAB206122) and Postgraduate Innovation special funds of Jiangxi Province (YC2018-S058).

References

[1] D. Luo, Z. Shen, Wetting and spreading behavior of borosilicate glass on Kovar, J. Alloy. Comp. 477 (1–2) (2009) 407–413.
[2] T.S. Chern, H.L. Tsai, Wetting and sealing of interface between 7056 Glass and Kovar alloy, Mater. Chem. Phys. 104 (2–3) (2007) 472–478.
[3] H.T. Lee, S.Y. Hu, T.F. Hong, Y.F. Chen, The shear strength and fracture behavior of Sn-Ag-*x*Sb solder joints with Au/Ni-P/Cu UBM, J. Electron. Mater. 37 (6) (2008) 867–873.
[4] P. Wang, D. Xu, Y. Zhai, The dissimilar brazing of Kovar alloy to SiCp/Al composites using silver-based filler metal foil, Appl. Phys. A 123 (9) (2017) 569.
[5] T.F. Song, X.S. Jiang, Z.Y. Shao, Interfacial microstructure and mechanical properties of diffusion-bonded joints of titanium TC4 (Ti-6Al-4V) and Kovar (Fe-29Ni-17Co) alloys, J. Iron Steel Res. Int. 24 (10) (2017) 1023–1031.
[6] J. Lu, Y. Mu, X. Luo, A new method for soldering particle-reinforced aluminum metal matrix composites, Mater. Sci. Eng.: A 177 (20) (2012) 1759–1763.
[7] J.W. Yoon, H.S. Chun, S.B. Jung, Liquid-state and solid-state interfacial reactions of fluxless-bonded Au-20Sn/ENIG solder joint, J. Alloy. Comp. 469 (1–2) (2009) 108–115.
[8] Y. Li, K. Luo, A.B.Y. Lim, Z. Chen, F.S. Wu, Y.C. Chan, Improving the mechanical performance of Sn57.6Bi0.4Ag solder joints on Au/Ni/Cu pads during aging and electromigration through the addition of tungsten (W) nanoparticle reinforcement, Mater. Sci. Eng.: A 669 (2016) 291–303.
[9] H.J. Lin, T.H. Chuang, Intermetallic reactions in reflowed and aged Sn-9Zn solder ball grid array packages with Au/Ni/Cu and Ag/Cu pads, J. Electron. Mater. 35 (1) (2006) 154–164.
[10] Y.C. Hsu, Y.M. Huang, C. Chen, Interfacial reaction and shear strength of Pb-free SnAg2.5Cu0.8Sb0.5 and SnAg3.0Cu0.5Sb0.2 solder bumps on Au/Ni(P) metallization, J. Alloy. Comp. 417 (1–2) (2006) 180–186.
[11] E.P. Lopez, P.T. Vianco, J.A. Rejent, Solderability testing of 95.5Sn-3.9Ag-0.6Cu solder on oxygen-free high-conductivity copper and Au-Ni-Plated Kovar, J. Electron. Mater. 32 (4) (2003) 254–260.
[12] J.W. Yoon, B.I. Noh, S.B. Jung, Interfacial reaction between Au-Sn solder and Au/Ni-metallized Kovar, J. Mater. Sci. Mater. Electron. 22 (1) (2011) 84–90.
[13] R.B. Cinque, J.W. Morris, The effect of gold-nickel metallization microstructure on fluxless soldering, J. Electron. Mater. 23 (6) (1994) 533–539.
[14] Q. Li, Y.C. Chan, Z. Chen, Interfacial microstructure and hardness of nickel (Ni) nanoparticle-doped tin-silver-copper (Sn-Ag-Cu) solders on immersion silver (Ag)-plated copper (Cu) substrates, J. Mater. Sci. Mater. Electron. 25 (9) (2014) 1222–1227.
[15] L.J. Yu, H.W. Yen, J.Y. Wu, J.J. Yu, C.R. Kao, Micromechanical behavior of singlecrystalline Ni_3Sn_4 in micro joints for chip-stacking application, Mater. Sci. Eng.: A 685 (2017) 123–130.
[16] X. Hu, T. Xu, L.M. Keer, Y. Li, X. Jiang, Shear strength and fracture behavior of reflowed Sn3.0Ag0.5Cu/Cu solder joints under various strain rates, J. Alloy. Comp. 690 (2017) 720–729.
[17] T.L. Yang, J.Y. Wu, C.C. Li, S. Yang, C.R. Kao, Low temperature bonding for high temperature applications by using SnBi solders, J. Alloy. Comp. 647 (2015) 681–685.
[18] X. Hu, W. Chen, X. Yu, Shear strengths and fracture behaviors of Cu/Sn37Pb/Cu soldered joints subjected to different displacement rate, J. Alloy. Comp. 600 (2014) 13–20.
[19] W. Liu, D.P. Sekulic, Capillary driven molten metal flow over topographically complex substrates, Langmuir 27 (11) (2011) 6720.
[20] W. Liu, Y. Li, Y. Cai, D.P. Sekulic, Capillary rise of liquids over a microstructured solid surface, Langmuir 27 (23) (2011) 14260.
[21] X. Hu, Y. Li, Y. Liu, Microstructure and shear strength of Sn37Pb/Cu solder joints subjected to isothermal aging, Microelectron. Reliab. 54 (8) (2014) 1575–1582.
[22] S. Ahat, M. Sheng, L. Luo, Microstructure and shear strength evolution of SnAg/Cu surface mount solder joint during aging, J. Electron. Mater. 30 (10) (2001) 1317–1322.
[23] X. Hu, N. Bao, Z. Min, Synergetic effect of strain rate and electroplated Cu film for shear strength of solder/Kovar joints, J. Mater. Sci. Mater. Electron. 30 (2019) 1434–1449.
[24] C. Yu, Y. Yang, J. Chen, Effect of deposit thickness during electroplating on Kirkendall voiding at Sn/Cu joints, Mater. Lett. 128 (2014) 9–11.
[25] C.E. Ho, L.H. Hsu, C.H. Yang, Effect of Pd(P) thickness on the soldering reaction between Sn-3Ag-0.5Cu alloy and ultrathin-Ni(P)-type Au/Pd(P)/Ni(P)/Cu metallization pad, Thin Solid Films 584 (2015) 257–264.
[26] R. Ghaffarian, CCGA packages for space applications, Microelectron. Reliab. 46 (12) (2006) 2006–2024.
[27] M. Yang, H. Ji, S. Wang, Effects of Ag content on the interfacial reactions between liquid Sn-Ag-Cu solders and Cu substrate during soldering, J. Alloy. Comp. 679 (2016) 18–25.
[28] K. Tokui, S. Sakuragi, T. Sasaki, Properties of sintered Kovar using metal injection molding, J. Jpn. Soc. Powder Powder Metall. 41 (6) (1994) 671–675.
[29] D.G. Kim, J.W. Kim, S.S. Ha, Effect of reflow numbers on the interfacial reaction and shear strength of flip chip solder joints, J. Alloy. Comp. 458 (1–2) (2008) 0–260.
[30] G. Zeng, S.D. Mcdonald, D. Mu, The influence of ageing on the stabilisation of interfacial $(Cu,Ni)_6(Sn,Zn)_5$ and $(Cu,Au,Ni)_6Sn_5$ intermetallics in Pb-free Ball Grid Array (BGA) solder joints, J. Alloy. Comp. 685 (2016) 471–482.
[31] C.Y. Yu, W.Y. Chen, J.G. Duh, Suppressing the growth of Cu-Sn intermetallic compounds in Ni/Sn-Ag-Cu/Cu-Zn solder joints during thermal aging, Intermetallics 26 (2012) 11–17.
[32] X. Hu, Y. Li, Z. Min, Interfacial reaction and IMC growth between Bi-containing Sn0.7Cu solders and Cu substrate during soldering and aging, J. Alloy. Comp. 582

(2014) 341–347.
[33] H. Li, R. An, C. Wang, Y. Tian, Z. Jiang, Effect of Cu grain size on the voiding propensity at the interface of SnAgCu/Cu solder joints, Mater. Lett. 144 (2015) 97–99.
[34] X. Hu, T. Xu, L. Keer, Microstructure evolution and shear fracture behavior of aged Sn3Ag0.5Cu/Cu solder joints, Mater. Sci. Eng.: A 673 (2016) 167–177.
[35] H.T. Lee, H.S. Lin, C.S. Lee, Reliability of Sn–Ag–Sb lead-free solder joints, Mater. Sci. Eng.: A 407 (1–2) (2005) 36–44.
[36] W. Liu, Y. Wang, Y. Ma, Interfacial microstructure evolution and shear behavior of Au–20Sn/(Sn)Cu solder joints bonded at 250°C, Mater. Sci. Eng.: A 651 (2016) 626–635.
[37] B. Lee, H. Jeon, K.W. Kwon, Employment of a bi-layer of Ni(P)/Cu as a diffusion barrier in a Cu/Sn/Cu bonding structure for three-dimensional interconnects, Acta Mater. 61 (18) (2013) 6736–6742.
[38] S.F. Choudhury, L. Ladani, Local shear stress-strain response of Sn-3.5Ag/Cu solder joint with high fraction of intermetallic compounds: experimental analysis, J. Alloy. Comp. 680 (2016) 665–676.
[39] W. Chen, S. Xue, H. Wang, J. Wang, Z. Han, Investigation on properties of Ga to Sn-9Zn lead-free solder, J. Mater. Sci. Mater. Electron. 21 (5) (2010) 496–502.
[40] S.M. Hayes, N. Chawla, D.R. Frear, Interfacial fracture toughness of Pb-free solder, Microelectron. Reliab. 49 (3) (2009) 269–287.